Analysis of the I3RC Two-Dimensional Step-Cloud Problem with TWODANT

Drew E. Kornreich, Anthony B. Davis, and Charles A. Rohde
Los Alamos National Laboratory
Technology Modeling and Analysis Group (TSA-7)
Space and Remote Sensing Sciences Group (NIS-2)

1. The Problem

The Intercomparison of 3D Radiation Codes (I3RC) modeling initiative includes one case that is relatively academic in nature. The geometry is an infinite series of clouds composed of two materials. The materials have the same microscopic scattering and absorbing properties, but the macroscopic properties vary according to material density. This is modeled as a two-cloud system with periodic boundary conditions (the exiting angular flux on the left face is equal to the entering angular flux on the right face) in *x*-*y* geometry (see **Figure 1**). Both clouds are 250 m wide (in the *x*-direction) and 250 m tall (in the *y*-direction) and infinite in extent in the *z*-direction. One cloud is 2 mean-free-paths (mfps) thick and the other is 18 mfps thick. The macroscopic total cross section for the diffuse and dense clouds are therefore 0.008 m^{-1} and 0.072 m^{-1}, respectively. Photons impinge the top of the clouds from a single direction.

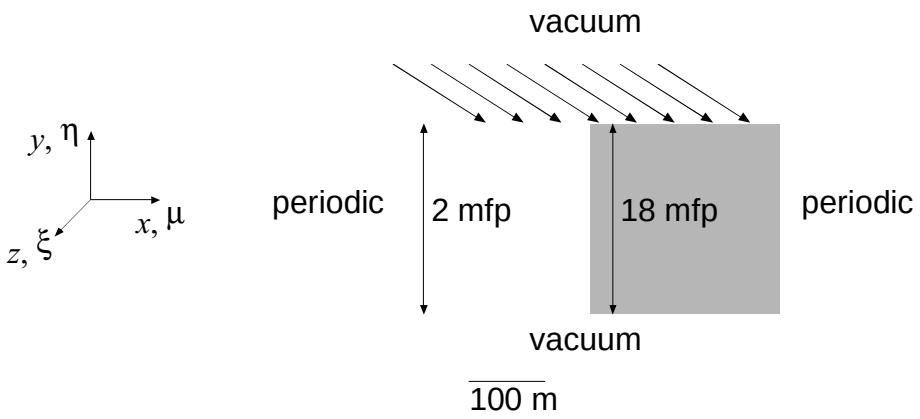

Figure 1. *Generic cloud geometry*.

2. DANTSYS

The DANTSYS[1] module of codes will be used in the analysis. DANTSYS was originally designed for nuclear engineering applications. Analyses of nuclear systems involve both neutron and photon particle transport through varied media. The DANT codes (ONEDANT, TWODANT, and THREEDANT) require input descriptions of the geometry, sources, and the absorbing and scattering properties of the materials. The

[1] R. E. Alcouffe, et al., DANTSYS: A Diffusion Accelerated Neutral Particle Transport Code System, LA-12969-M, Los Alamos National Laboratory (1995).

DANT codes were designed to solve the stationary Boltzmann equation. The codes can be used for multigroup (particle energy dependent) problems; however, the two-cloud problem assumes all particles originate and remain at the same energy (or wavelength). The codes use the discrete-ordinates method for discretizing the angular variable over the unit sphere.

2.1. Cloud Geometry

The geometry shown in **Figure 1** is clearly best modeled using a two-dimensional Cartesian geometry; therefore, we will use the TWODANT module. A small series of clouds is modeled to avoid using periodic boundary conditions (currently problematic with TWODANT). Results from the central clouds will be used, with adjacent clouds present to mimic the periodicity of the geometry. The geometry used for the TWODANT input is shown in **Figure 2**. The numbers of mesh intervals in the two directions are shown for each slab. Vacuum boundary conditions are used for all external surfaces.

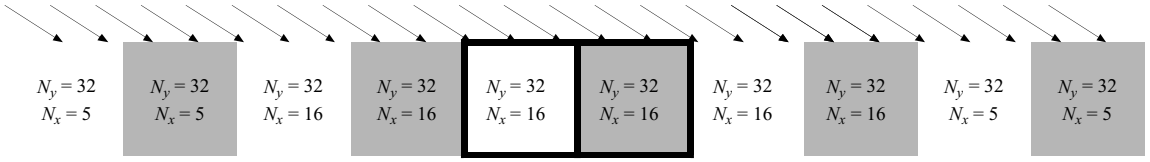

Figure 2. *TWODANT model cloud geometry*.

The angular variable is discretized by using the S_{100} triangular Chebychev-Legendre quadrature set.[2] This results in 5100 discrete angles in the unit hemisphere (only need a hemisphere in two-dimensional Cartesian geometry). This quadrature order is the maximum allowable by the code before the user must supply the quadrature constants; the maximum number of angles is used because the scattering properties will be very forward-peaked, indicating that the number of possible scattering angles should be as large as possible.

2.2. Cross Sections

The problem consists of four different cases — two incident source angles and two different absorbing properties of the medium. However, in all cases, the scattering properties are given in terms of a Henyey-Greenstein phase function:

$$p(\mu) = \frac{1}{4\pi} \frac{1-g^2}{\left[1+g^2-2g\mu\right]^{3/2}} \quad . \tag{1}$$

Note that for $g = 0$, we have isotropic scatting, and in the limit as g approaches 1 we have purely forward scattering. In this section, we derive the required cross section input based on the approximation of the scattering cross sections as finite Lengendre polynomial expansions. The scattering cross section for neutral particles is written in terms of a Lengendre polynomial expansion as

[2] O Dell R. D. and R. E. Alcouffe, Transport Calculations for Nuclear Analysis: Theory and Guidelines for Effective Use of Transport Codes, Los Alamos National Laboratory, LA-10983-MS, September 1987.

$$\sigma_s(\mathbf{r},\Omega\cdot\Omega') = \sigma_s(\mathbf{r},\mu) = \sum_{l=0}^{\infty} \frac{2l+1}{4\pi}\sigma_s^l(\mathbf{r})P_l(\mu) \tag{2}$$

Multiplying both sides of the equation by $P_m(\mu)$ and integrating over the range of Legendre polynomials gives us the moments as (after using the Legendre polynomial orthogonality properties)

$$\sigma_s^m(\mathbf{r}) = 2\pi\int_{-1}^{1} d\mu\sigma_s(\mathbf{r},\mu)P_m(\mu) \quad . \tag{3}$$

We assume that the scattering cross section is given in terms of two separable functions - the Henyey-Greenstein phase function and the composite scattering cross section, which is only a function of position:

$$\sigma_s^m(\mathbf{r}) = 2\pi\sigma_s(\mathbf{r})\int_{-1}^{1} d\mu p(\mu)P_m(\mu) \quad . \tag{4}$$

Performing the above integral yields

$$\int_{-1}^{1} d\mu p(\mu)P_m(\mu) = \frac{1}{2\pi}g^m \quad . \tag{5}$$

Thus, the scattering cross section moments for all orders are

$$\sigma_s^m(\mathbf{r}) = \sigma_s(\mathbf{r})g^m \quad . \tag{6}$$

The above derivation is exact if the upper limit of the sum in Eq. (2) is infinite. In practice, we approximate the scattering cross section by truncating the series at some upper limit L. A graphical display of the scattering orders required to accurately represent a Henyey-Greenstein phase function with $g = 0.85$ is shown in **Figure 3** for a few angles μ ($\mu = 1$ is the forward direction and $\mu = -1$ is the backward direction). The percent relative error in the scattering cross section $\sigma_s(\mathbf{r},\Omega\cdot\Omega')$ is given by

$$\%\text{Relerr}(\mu) = 100\times\frac{\sigma_s(\mathbf{r})p(\mu) - \sigma_s(\mathbf{r})\sum_{l=0}^{L}\frac{(2l+1)}{4\pi}g^l P_l(\mu)}{\sigma_s(\mathbf{r})p(\mu)} \quad . \tag{7}$$

Large errors are seen for back-scattering. Given our limit of S_{100} scattering, the effective limit on the scattering order approximation is 50 to allow for accurate integration of the higher order flux moments. The results shown in **Figure 3** seem to indicate that obtaining accurate results at an approximation level of 50 scattering orders will be hopeless. However, we will be analyzing systems that have very forward-peaked

scattering properties, and the largest errors in approximating the scattering properties are for the backward directions.

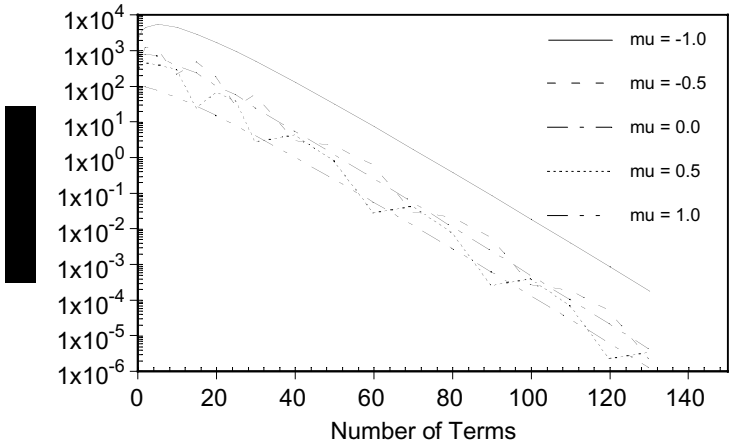

Figure 3. *Partial sum errors for a Henyey-Greenstein phase function*, $g = 0.85$. The ordinate is relative error in %.

To estimate the effect of scattering order on results, we examine the I3RC case with a mean number of secondaries of 0.99 and normal photon incidence. A TWODANT run was performed with higher-order scattering cross sections up to $L = 50$. The results are shown in **Table 1**. As can be seen from the table, after L increases beyond 15, very little change appears in the final result. Thus, for all cases analyzed here, we use $L = 25$ as the scattering order approximation for a Henyey-Greenstein phase function with $g = 0.85$.

Thus, the cross section file is composed of a total cross section for each material plus a list of all scattering cross section orders, which are given by

$$\sigma_s^m(\mathbf{r}) = \sigma_t(\mathbf{r})c(\mathbf{r})g^m \quad , \tag{8}$$

where c (denoted as the single-scatter albedo, ϖ_0, in the radiative transfer community) is the number of secondary particles emitted per collision ($c = 0.99$ and $c = 1.00$ are the two cases investigated here).

2.3. Source Description

As mentioned, the set of four cases is a combination of two scattering descriptions and two source incidence angles. One case involves normal incidence on the top surface and the second involves a uniform canted beam on the top surface. Using the coordinate axes shown in **Figure 1**, we see that normal beam incidence is described by angle unit vector components $\mu = 0$, $\eta = -1$, $\xi = 0$. The canted beam case has the beam impinging normal to the z-axis at an angle of 60 degrees below the vertical direction. This source is described by the directional angle unit vector components $\mu = 0.866$, $\eta = 0.5$, $\xi = 0$.

Boundary angular sources in TWODANT must be along one of the S_N directions. The discrete angles that most closely match these source directions are

Normal beam: direction 1275; μ = -0.015705, η = -0.99975, ξ = 0.015629
Canted beam: direction 2517; μ = 0.86853, η = -0.49540, ξ = 0.015629

Photons illuminate all mesh cells on the top surface from the directions specified above.

Table 1. *Albedo and Transmission for the c* = 0.99*, normal incidence case*.

L	Albedo	Transmission	*L*	Albedo	Transmission
0	0.61947	0.23812	10	0.26109	0.59748
1	0.22722	0.59865	11	0.26193	0.59697
2	0.23337	0.61998	12	0.26140	0.597215
3	0.27170	0.59757	13	0.26108	0.59739
4	0.26522	0.59458	14	0.26133	0.59728
5	0.25512	0.60042	15	0.26154	0.59717
6	0.25894	0.59922	25	0.26133	0.59729
7	0.26292	0.59685	50	0.26134	0.59728
8	0.26163	0.59713			
9	0.260218	0.59788			

3. Results

TWODANT is run using the input parameters described above to a convergence criterion of 1×10^{-5}. Particle balance tables print the upward and downward currents at each mesh cell. The albedo of a given top mesh cell is given by dividing the upward current (return current off the top face) by the downward current (the source). Averaging these cell albedos over the two clouds highlighted in **Figure 2** gives the mean albedo, *R*. The cell transmission is likewise given by dividing the downward current in the bottom cell (transmitted current off the bottom face) by the downward cell current at the top of the cloud (the source) and then averaging all cell transmission factors to obtain a mean transmission, *T*. We obtain the column absorptance by summing the cell absorptances at each position *x* and dividing by the incident source on that cell. The mean absorptance, *A*, is derived simply by averaging the column absorptances over the two clouds. The mean net horizontal flux, *H*, is obtained by averaging the cell net horizontal fluxes [$H(x)$˚= 1 — (x) —$R(x)$ —$A(x)$]. If the boundary conditions are truly periodic, the mean net horizontal flux through the two-cloud system, *H*, should be zero. Again, periodic boundary conditions hold that the exiting flux on the left face is equal to the entering flux on the right face, thereby giving a mean net horizontal flux of zero.

The results of the mean quantity calculations are shown in **Table 2**. **Table 2** also contains a list of the computer run times for each case. All TWODANT cases were run on a Sparc Ultra 2 (two processors) with 2 GB of internal memory. TWODANT is not configured to use both processors; however, the second processor mitigates competition

for processor time between these code calculations and system processes or other code processes.

Table 2. *Step Cloud: TWODANT Average Quantity Results*.

Case	R	T	A	H	Run Time (hr)
SZA = 0, c = 0.99	0.2613	0.5973	0.1412	0.0001	19.4
SZA = 0, c = 1.00	0.3280	0.6716	0.0000	0.0004	22.2
SZA = 60, c = 0.99	0.4786	0.3227	0.1984	0.0003	20.1
SZA = 60, c = 1.00	0.5825	0.4170	0.0000	0.0007	22.9

We now look at the columnar quantities in the cloud system. **Figure 4** graphically displays the columnar quantities in the cloud system. Note again from **Figure 1** that the diffuse (less dense) cloud is on the left ($0 < x < 250$ m) and the dense cloud is on the right ($250 \text{ m} < x < 500$ m). As expected, the albedos are larger for the cases with $c = 1.00$ than for those with $c = 0.99$. The transmitted flux out the bottom of the cloud is larger for the diffuse cloud because more photons are able to pass through this medium. However, the albedos are larger for the dense cloud because more scattering occurs in this cloud, thereby giving the photons a chance to return upward. The shifting of the peak flux as a result of the canted beam is also readily apparent the graphs. The absorption in the denser cloud is clearly evident, as is the effect of curve shifting that results from a canted beam.

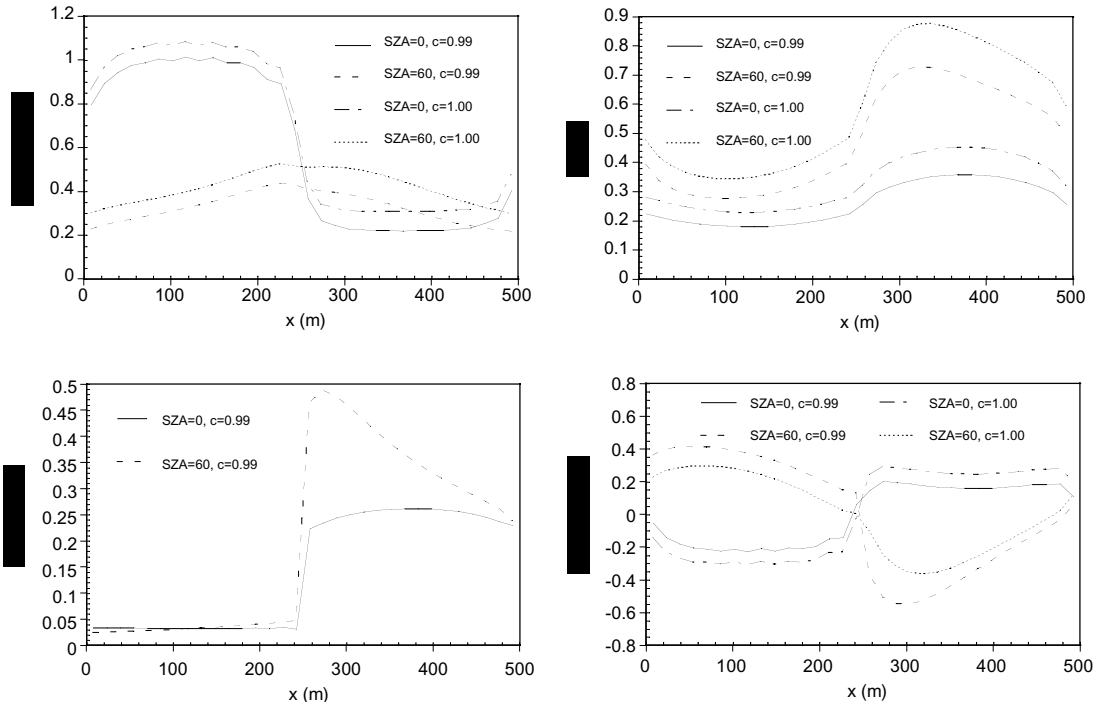

Figure 4. *Graphical results as a function of position.* Clockwise from upper-left: transmitance, reflectance (albedo), horizontal fluxes, absorptance.

Evident in the above graphs are a few curves that have oscillations. This is a typical artifact of a discrete ordinates code. Decreasing the mesh spacing usually removes (or reduces) these oscillations that often occur in beam source problems. In general, these oscillations appear in the diffuse medium where little scattering is available to disperse the angularly singular source.

4. Conclusions

From the above results, TWODANT was able to adequately model the cloud system. However, not all results requested for the I3RC modeling effort were available from TWODANT. No results that require analysis of the angular flux exiting the clouds (the radiance fields) are available because of a coding error that produces inaccurate results when the card that writes the boundary angular fluxes is active. A possible alternative is to use the THREEDANT code to model the two-dimensional system (with hope that this error was eliminated), but using a three-dimensional code will increase the computational resource requirements. An additional advantage of using THREEDANT is that the angular source is not restricted to one of the S_N directions, although we are using enough directions to approximate the sources fairly well.

In addition, some work to examine the effect of the geometric mesh spacing could reduce oscillations in the results that were seen in the graphs. Another parameter that was held constant in this analysis was S_N. It might be of some interest to examine sensitivity to the angular quadrature order for this suite of problems.

This I3RC modeling effort has been a good test for TWODANT. Notwithstanding the two coding errors uncovered (inaccurate results with periodic boundary conditions specified and the card associated with writing the boundary angular fluxes), TWODANT was able to produce accurate results for the mean quantities requested. Also, the nuclear engineering application for which the DANTSYS codes are used generally approximate the scattering at much lower levels ($L < 10$). Clearly, the DANTSYS codes can also be used for classes of problems that have severe forward-peaked scattering.